The Aerodynamics of Heavy Vehicles II: Trucks, Buses, and Trains, **Lecture Notes in Applied and Computational Mechanics**, Volume 41, 151-160, 2009. Springer Berlin Heidelberg.

Adaptive Control of Post-Stall Separated Flow

Application to Heavy Vehicles

[1]Louis N. Cattafesta III, [1]Ye Tian and [2]R. Mittal

[1]Interdisciplinary Microsystems Group
Department of Mechanical and Aerospace Engineering
Gainesville, FL 32611-6250

[2]Department of Mechanical and Aerospace Engineering
The George Washington University
Washington, DC 20052.

Abstract This paper discusses two adaptive feedback control approaches designed to reattach a massively separated flow over a NACA airfoil with minimal control effort using piezoelectric synthetic jet actuators and various sensors for feedback. One approach uses an adaptive feedback disturbance rejection algorithm in conjunction with a system identification algorithm to develop a reduced-order dynamical systems model between the actuator voltage and unsteady surface pressure signals. The objective of this feedback control scheme is to suppress the pressure fluctuations on the upper surface of the airfoil model, which results in reduced flow separation, increased lift, and reduced drag. A second approach leverages various flow instabilities in a nonlinear fashion to maximize the lift-to-drag ratio using a constrained optimization scheme – in this case using a static lift/drag balance for feedback. The potential application of these adaptive flow control techniques to heavy vehicles is discussed.

Introduction

Flow separation incurs a large amount of energy loss and limits the performance of many flow-related devices (e.g., airfoils, automobiles, trucks etc.). Researchers have been trying to mitigate or eliminate flow separation for over a century because of its large potential payoff in practical applications. Numerous passive and active separation control strategies have been attempted with varying degrees of success. Passive techniques involve geometric modifications to alter the flow characteristics, while active methods involve the use of flow actuators to modify the flow and therefore require external energy addition.

Passive techniques are desirable because of their simplicity and, if properly designed, their effectiveness at design conditions. However, the performance of a passive control system usually degrades at off-design conditions. In the context of heavy vehicles, "off-design" encompasses speed deviations and poor weather (e.g., wind, snow, or rain).

The main benefit of active techniques is their ability to "adapt" to off-design conditions. However, most of the active control approaches are open-loop in nature and, hence, are not really adaptive. Feedback control uses sensors to feed back information about the flow and/or vehicle states, and a controller automatically adjusts the actuator input to achieve a desired control objective. If the controller is adjusted or redesigned automatically during this process, it is called "adaptive." The primary disadvantage of this approach is its complexity, and its use thus represents a paradigm shift from conventional passive and active control. Nonetheless, the potential performance benefits and improved robustness warrants research.

This paper addresses a model problem that is representative of the separated flow behind a heavy vehicle. In particular, two adaptive feedback control approaches are discussed that seek to reattach a massively separated flow over a NACA 0025 airfoil with minimal control effort using piezoelectric zero-net mass-flux actuators and various sensors for feedback. One approach uses an adaptive feedback disturbance rejection algorithm in conjunction with a system identification algorithm to develop a reduced-order dynamical systems model between the actuator voltage and unsteady surface pressure signals. Its objective is to suppress the pressure fluctuations on the upper surface of the airfoil model, which results in reduced flow separation, increased lift, and reduced drag. A second approach leverages various convective and global flow instabilities in a nonlinear fashion to maximize the lift-to-drag ratio using a constrained optimization scheme – in this case using a static lift/drag balance for feedback. Experiments are described to elucidate the baseline uncontrolled and controlled flow physics, and the potential application of these approaches to heavy vehicles is discussed.

Experimental Configuration

As shown in Fig. 1, separation control experiments are conducted on a two-dimensional, $c = 15.24$ cm chord NACA 0025 airfoil mounted in an open-return, low-speed wind tunnel with a 30.48 cm by 30.48 cm by 60.96 cm test section. Six unsteady pressure transducers (Kulite LQ125-5A) are mounted beneath 2.2 mm diameter pinhole apertures at the mid-span location located at approximately 44.0%, 52.5%, 61.0%, 69.5%, 77.9% and 86.4% chord. A strain-gauge balance integrated into the model mount is used to measure the total lift and drag forces of the airfoil for varying angles of attack.

The airfoil contains four piezoelectric zero-net mass-flux (ZNMF) actuators with $h = 0.5$ mm wide slots located in the central 1/3rd spanwise region of the air-

foil. Here we describe control experiments that only use actuator #1 located at the 3% chord location; the other unused actuators slots are covered. Details on the synthetic jet actuators used in this research can be found in Gallas et al. (2003), Holman et al. (2003), and Gallas (2005).

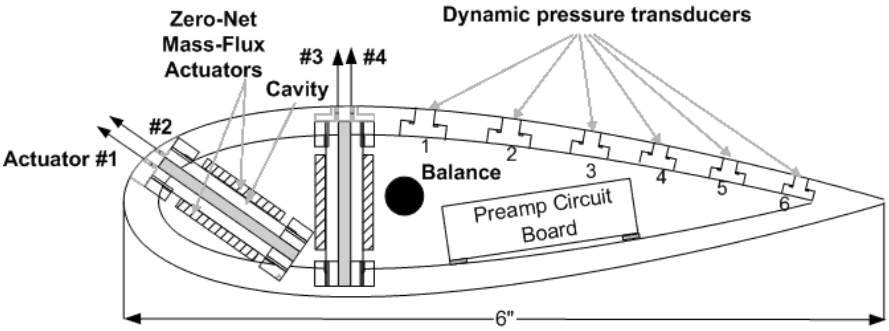

Fig. 1. Experimental setup of NACA 0025 airfoil showing four ZNMF actuators, a strain gage balance, and six dynamic surface pressure transducers.

The control system for the separation control experiments is implemented using a dSPACE (Model DS1005) DSP system with a 466 MHz PowerPC CPU. The dSPACE system has a 5-channel 16-bit A/D board (DS2001) and a 6-channel 16-bit D/A board (DS2102). The control algorithms are first programmed in Matlab/Simulink and C programs (C code S-functions) and then compiled and loaded on the dSPACE DSP processor.

The angle of attack (AoA) was greater than 10° for these experiments, corresponding to massive leading-edge separation or post-stall separated flow, as shown in Fig. 2. The chord Reynolds number, $\mathrm{Re}_c = \rho U_\infty c/\mu$, was 1E5 to 1.2E5. The BL is tripped in the leading edge region using 100 sand grit.

Problem Definition and Background

The objective of the control is to reattach the flow to the airfoil surface with minimal actuator power expenditure. A ZNMF actuator is a popular device for active flow control that requires no external flow source and works by alternately expelling and ingesting fluid through the actuator slot via a vibrating diaphragm (Glezer and Amitay 2002). Input sinusoidal oscillations are characterized by a dimensionless frequency $F^+ = fc/U_\infty$ and oscillatory momentum coefficient, $< C_\mu >= \left(\rho u_{j,rms}^2 h\right) \Big/ \left(0.5\rho U_\infty^2 c\right)$, where $u_{j,rms}$ is the rms jet velocity in the slot.

Although numerous studies are reported in the literature to determine the optimal forcing frequencies for effective separation control, the observed values of optimal F^+ vary over a wide range. For example, Greenblatt and Wygnanski (2000)

concluded that the optimal range is $2 < F^+ < 4$. Seifert and Pack (1999) found that the excitation frequency should be chosen such that $0.5 < F^+ < 1.5$ over a wide range of high Reynolds numbers. Conversely, Amitay et al. (2001) found that when the excitation frequency $F^+ > 10$, the lift-to-pressure-drag ratio was larger than when the excitation frequency $F^+ < 4$ for their unconventional airfoil.

Fig. 2. Instantaneous laser light sheet visualization of the baseline uncontrolled post-stall separated flow on the airfoil at Re_c = 1E5 and angle-of-attack (AoA) = 20°.

For the case shown in Fig. 2, the optimal open-loop sinusoidal forcing for the present experiment is F^+=15 with $< C_\mu >= 3.16 \times 10^{-4}$, resulting in partial reattachment with an increase in lift-to-drag ratio from 1.1 for the baseline uncontrolled case to 1.76 (Tian 2007). Thus, it may appear that the present results are more in line with the findings of Amitay et al. However, this result is misleading since the optimal value of F^+ depends not only on the flow dynamics but also on the actuator. Fig. 3 shows the normalized frequency response (i.e., the ratio of output rms jet velocity to input sinusoidal voltage) of actuator 1. Note that the actuator output is negligible below 500 Hz and peaks around 1100 Hz. So the optimal result of F^+=15, which corresponds to ~1000 Hz excitation, is at least partially explained by the fact that the actuator "works best" near this frequency. Nonetheless, the goal of the closed-loop control schemes is to at least match the performance of this optimal open-loop result, preferably with reduced actuator output, by relaxing the restriction to sinusoidal excitation.

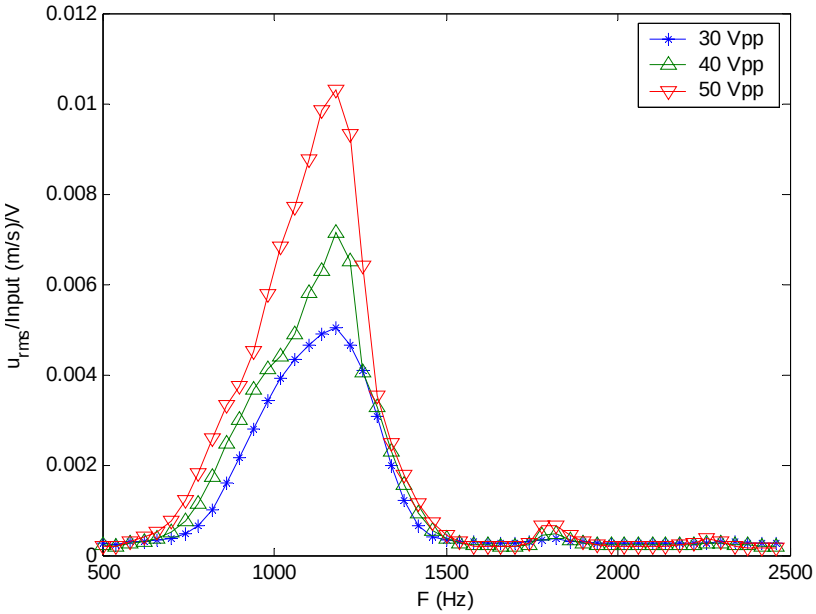

Fig. 3. Frequency response of ZNMF actuator 1. Note the actuator produces non-negligible output to sinusoidal inputs only in the range from 500-1500 Hz.

Results and Discussion

In this section we summarize the results for two algorithms used for real-time adaptive flow control. The first is a conventional adaptive disturbance rejection algorithm that includes an adaptive linear system identification model. The second approach uses a nonlinear constrained optimization strategy to adjust the parameters of a multi-frequency waveform to maximize the lift-to-drag ratio.

ARMARKOV Disturbance Rejection

As mentioned above, this algorithm contains two parts: system identification (ID) and control. The ID portion produces a low-order dynamical system model between the actuator voltage and the unsteady pressure signals, while the control algorithm seeks to suppress the power or mean-square value of the unsteady pressure fluctuations from one of the transducers. This approach is based on an inherent assumption that the unsteady pressure fluctuations are larger when the flow is

separated due to the passage of vortical structures over the surface of the model, the validity of which is demonstrated in Kumar and Alvi (2005).

A block diagram of the simultaneous ID and control algorithm is shown in Fig. 4. Here, both ID and control signals are input into the flow system, comprised of the actuator and airfoil, and the outputs of the system are assumed to be unsteady surface pressure measured by the transducers. The ID algorithm uses a band-limited input signal to the actuator with the performance pressure signal to develop an ARMARKOV system ID model (Akers and Bernstein 1997). The adaptive disturbance rejection algorithm uses the parameters identified in the system model combined with the measured airfoil surface pressures to tune or adjust the controller (Venugopal and Bernstein 2000). The ID and disturbance rejection algorithms are described in detail in the above references and in Tian et al. (2006b) and Tian (2007) for this problem.

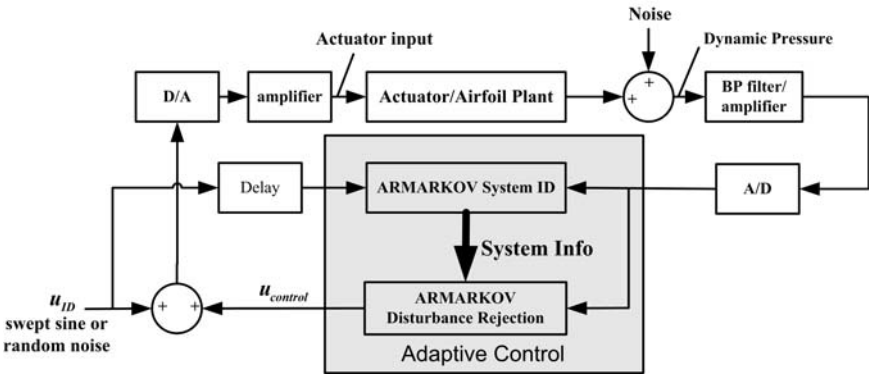

Fig. 4. Block diagram of adaptive system identification and disturbance rejection algorithm.

Constrained Nonlinear Optimization

Various optimization strategies are discussed in the literature (Press et al. 1992). After some experimentation with several extremum-seeking algorithms (Artiyur and Krstic 2003; Banaszuk et al. 2003), the downhill simplex method described in Press et al. was implemented to minimize the drag-to-lift ratio.

The benefits of the algorithm are its simplicity and applicability to multi-parameter constrained optimization and its faster convergence rate compared to extremum-seeking control for the present problem. The key steps of the algorithm are summarized as follows: 1) evaluate the cost function at chosen initial conditions, 2) use the lowest value as a reference and search for a lower value of the cost function, 3) move only in the downhill direction, and 4) terminate when some convergence criteria are met. The method thus finds a local minimum. To improve the probability of finding the global minimum, multiple experiments are

performed starting from different initial conditions. Again, the details of this algorithm are described in Tian et al. (2006a) and Tian (2007).

As explained in Tian (2007), the separated flow exhibits two dominant flow instabilities. The separated shear layer is characterized by convective Kelvin-Helmholtz (K-H) instabilities, which manifest themselves as the large-scale vortical structures with frequency $f_{SL} \sim U_\infty / \theta_0$, where θ_0 is the initial momentum thickness of the boundary layer just prior to separation (see Fig. 2). The large wake is characterized by a global instability, which manifests itself as a vortex street with frequency $f_{wake} \sim U_\infty / \theta_{wake}$, where θ_{wake} is the momentum thickness of the wake. The global wake instability interacts in a nonlinear fashion with the K-H instability. Since $\theta_{wake} >> \theta_0$, then $f_{wake} << f_{SL}$ so these two frequencies are widely separated in the post-stall case. This fact emphasizes the need for an actuator with sufficient bandwidth to excite both instabilities. The key assumption is that control will be more effective if both of these instabilities are excited, and this can only be achieved via a mult-frequency waveform.

Tian et al. (2006a) and Tian (2007) describe three such waveforms: amplitude modulation (AM), burst modulation (BM), and pulse modulation (PM). Each of these represents the product of a high-frequency carrier signal and a low-frequency modulation signal. For example, an AM signal is

$$e(t) = A \sin\left(2\pi f_c t\right) \frac{1 + \sin\left(2\pi f_m t\right)}{2},$$

which is characterized by three parameters: the amplitude A, carrier frequency f_c, and modulation frequency f_m. The use of such a complex waveform produces a rich spectrum of input disturbances due to flow nonlinearities, which in turn excites the K-H and wake instabilities. The goal of the simplex algorithm is to adjust these three parameters to minimize the drag-to-lift ratio.

Finally, to negate the preferential actuator output over a certain frequency range described above, the ZNMF actuator output jet rms velocity is "calibrated" using a constant-temperature hot-wire anemometer and current probes for each waveform type (AM, BM, or PM) to provide a look-up table that relates $< C_\mu >$ and actuator electrical power to the waveform parameters. In this manner, the optimization can be constrained to fix either $< C_\mu >$ or electrical power while A, f_c, and f_m are adjusted. This permits a fair comparison between different actuator waveforms.

Both adaptive controllers are able to completely reattach the separated flow at AoA=12°, as shown in Fig. 5, and L/D is increased to 7.0 ± 0.4. As the AoA is increased above 12°, the performance of the adaptive disturbance rejection controller, which is inherently linear, gradually deteriorates. Finally at AoA=20°, the lift-to-drag ratio is essentially identical to that of the uncontrolled case ($L/D = 1.1 \pm 0.04$). In contrast, the nonlinear controller is more robust at higher

angles of attack. In particular, at AoA=20°, $L/D = 2.18 \pm 0.07$ for AM with $< C_\mu >= 7.15 \times 10^{-6}$, $f_m = 61$ Hz and $f_c = 2405$ Hz. Optimal sinusoidal control was achieved with $< C_\mu >= 3.16 \times 10^{-4}$, resulting in $L/D = 1.76 \pm 0.03$. Note that slightly superior performance is achieved via nonlinear feedback vs. sinusoidal control but with a reduction in $< C_\mu >$ by a factor of 44! More details on these experiments are provided in Tian (2007).

Conclusions

The results of these experiments on a model post-stall airfoil problem show the potential of adaptive control of separated flow. In particular, the nonlinear controller appears most promising due to its ability to leverage multiple flow instabilities and therefore achieve control with very low energy expenditure.

The above closed-loop methodology appears to be applicable to heavy vehicles and would be a natural extension of previous open-loop control approaches (Hsu et al. 2004; Englar 2004). In particular, the massive wake behind a truck will likely exhibit similar flow instabilities as that of a post-stall airfoil, namely the K-H shear layer and global wake instabilities. Of course, the three-dimensional nature of the bluff body wake will be more complex. In addition, the objective function for control will differ from the lift-to-drag ratio. Since drag reduction is the main objective for a heavy vehicle, maximizing the average base pressure is perhaps a reasonable objective. Unsteady actuation around the rear perimeter of the vehicle appears to be a logical location for the actuators. In summary, it seems clear that further research on this topic is both warranted and required to understand the benefits and limitations of adaptive feedback flow control as applied to heavy vehicles.

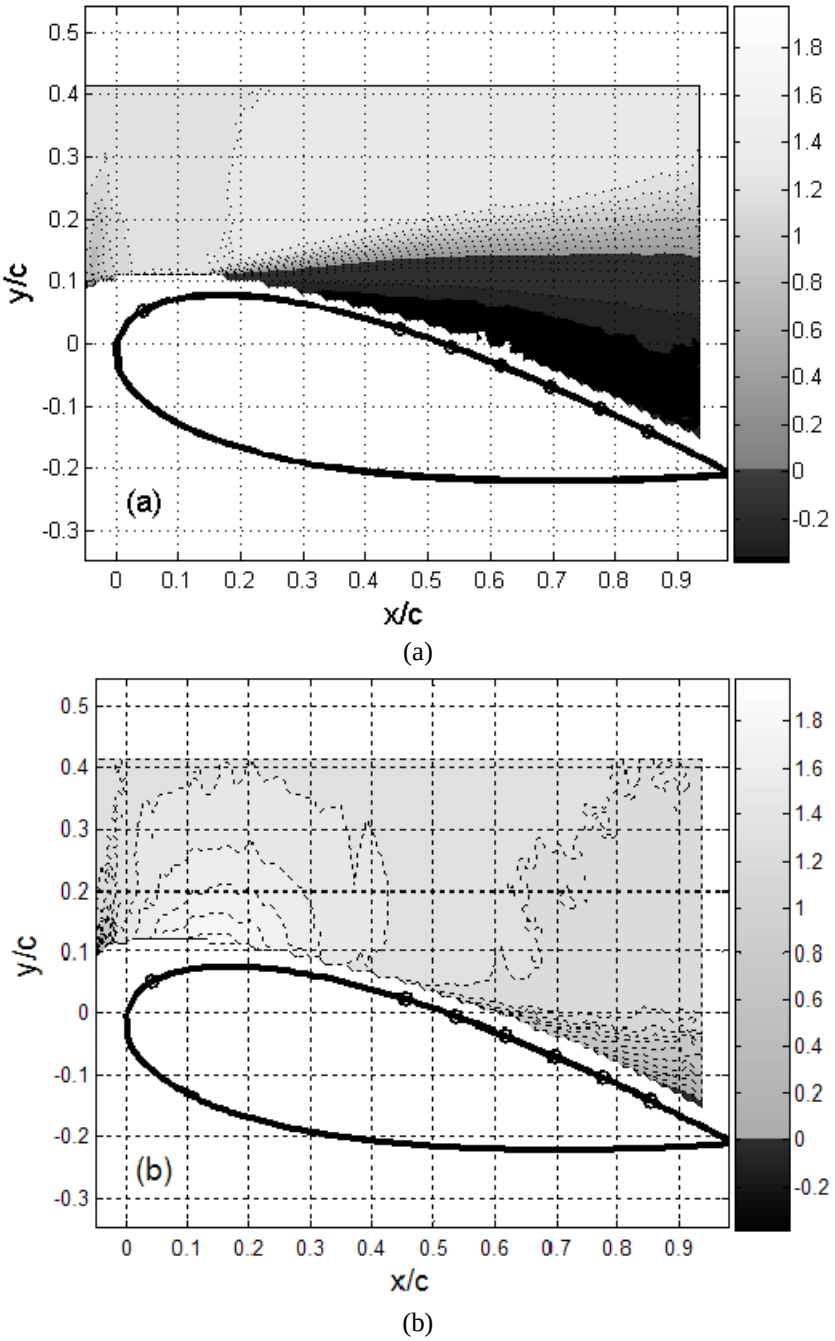

Fig. 5. Contours of streamwise velocity u/U_∞ for (a) baseline and (b) closed-loop control at AoA = 12° and Re_c =120,000.

References

Akers, J. C. and Bernstein, D. S., "Time-Domain Identification Using ARMARKOV/Toeplitz Models", Proceedings of the American Control Conference, pp. 191-195, June 1997.

Amitay, M., Smith, D., Kibens, V., Rarekh, D. and Glezer A., "Aerodynamic Flow Control over an Unconventional Airfoil Using Synthetic Jet Actuators," *AIAA Journal*, Vol. 39, No. 3, pp. 361-370, March 2001.

Artiyur, K. B. and Krstic, M., Real-Time Optimization by Extremum-Seeking Control, Wiley-Interscience, 2003.

Banaszuk, A., Narayanan S. and Zhang Y., "Adaptive Control of Flow Separation in a Planar Diffuser," AIAA paper 2003-0617, January 2003.

Englar, R., "Pneumatic Heavy Vehicle Aerodynamic Drag Reduction, Safety Enhancement and Performance Improvement," Proceedings of the UEF Conference on The Aerodynamics of Heavy Vehicles:Trucks, Buses and Trains, Lecture Notes in Applied and Computational Mechanics Springer-Verlag, Heidelberg, September, 2004.

Gallas, Q., "On the Modeling and Design of Zero-Net Mass Flux Actuators," Ph.D. Thesis, Department of Mechanical and Aerospace Engineering, University of Florida, May 2005.

Gallas, Q., Holman, R., Nishida, T., Carroll, B., Sheplak, M., and Cattafesta, L., "Lumped Element Modeling of Piezoelectric-Driven Synthetic Jet Actuators," *AIAA Journal*, Vol. 41, No. 2, pp. 240-247, 2003.

Glezer, A. and Amitay, M., "Synthetic Jets," *Annual Review of Fluid Mechanics*, Volume 34, pp. 503-529, January 2002.

Greenblatt, D and Wygnanski, I, "The control of flow separation by periodic excitation," *Progress in Aerospace Sciences*, Vol. 36, pp. 487-545, 2000.

Holman, R., Quentin, G., Carroll, B. and Cattafesta, L., "Interaction of Adjacent Synthetic Jets in an Airfoil Separation Control Application", AIAA Paper 2003-3709, June 2003.

Hsu, T-Y., Hammache, M. & Browand, F., "Base Flaps and Oscillatory Perturbations to Decrease Base Drag," Proceedings of the UEF Conference on The Aerodynamics of Heavy Vehicles:Trucks, Buses and Trains, Lecture Notes in Applied and Computational Mechanics Springer-Verlag, Heidelberg, September, 2004.

Kumar, V. and Alvi, F. S., "Efficient Control of Separation Using Microjets," AIAA Paper 2005-4879, June 2005.

Press, W. H., Flannery, B. P., Teukolsky, S. A. and Vetterling, W. T., Numerical Recipes in Fortran, 2nd edition, Cambridge University Press, January 1992.

Seifert, A., Pack, L. G., "Oscillatory Control of Separation at High Reynolds Numbers," *AIAA Journal*, Vol. 37, No. 9, pp. 1062-1071, September 1999.

Tian, Y., "Adaptive Control of Separated Flow," Ph.D. Thesis, Department of Mechanical and Aerospace Engineering, University of Florida, Gainesville, FL, August 2007.

Tian, Y., Cattafesta, L., and Mittal, R. "Adaptive Control of Separated Flow," AIAA Paper 2006-1401, January 2006a.

Tian, Y., Song, Q., and Cattafesta, L., "Adaptive Feedback Control of Flow Separation," AIAA Paper 2006-3016, June 2006b.

Venugopal, R. and Bernstein D. S., "Adaptive Disturbance Rejection Using ARMARKOV/Toeplitz Models," IEEE Transactions on Control Systems Technology, Vol. 8, No. 2, pp. 257-269, March 2000.